CrossMark

Pre-processing and transfer entropy measures in motor neurons controlling limb movements

Fernando P. Santos[1,2] · Carlos D. Maciel[1] · Philip L. Newland[3]

Abstract Directed information transfer measures are increasingly being employed in modeling neural system behavior due to their model-free approach, applicability to nonlinear and stochastic signals, and the potential to integrate repetitions of an experiment. Intracellular physiological recordings of graded synaptic potentials provide a number of additional challenges compared to spike signals due to non-stationary behaviour generated through extrinsic processes. We therefore propose a method to overcome this difficulty by using a preprocessing step based on Singular Spectrum Analysis (SSA) to remove nonlinear trends and discontinuities. We apply the method to intracellular recordings of synaptic responses of identified motor neurons evoked by stimulation of a proprioceptor that monitors limb position in leg of the desert locust. We then apply normalized delayed transfer entropy measures to neural responses evoked by displacements of the proprioceptor, the femoral chordotonal organ, that contains sensory neurones that monitor movements about the femoral-tibial joint. We then determine the consistency of responses within an individual recording of an identified motor neuron in a single animal, between repetitions of the same experiment in an identified motor neurons in the same animal and in repetitions of the same experiment from the same identified motor neuron in different animals. We found that delayed transfer entropy measures were consistent for a given identified neuron within and between animals and that they predict neural connectivity for the fast extensor tibiae motor neuron.

Keywords Synaptic responses · Neural network · Information theory · Singular spectrum analysis · Analogue signals

1 Introduction

One key advantage of *Information Theoretic* approaches is that they provide tools capable of analyzing nonlinear and stochastic signals in a model-free approach (Ebeling 2002). Moreover, information transfer measures, such as mutual information (Wilmer et al. 2012) and transfer entropy (Schreiber 2000; Wollstadt et al. 2014), can be employed to propose network structures capable of explaining complex systems by providing a model, not just in function of an input-output response, but also with dynamic internal states that interact. This type of model is referred to as a Dynamic Bayesian Network (Smith et al. 2006).

In this context, here we develop and apply these tools to the analysis of connectivity and information transfer in neural networks responsible for controlling limb movements. This area has become increasingly a focus of research, not simply to understand how movements are produced and controlled by the nervous system, but also for their potential applicability in bioinspired robotics and neuroprotheses design. Insect sensorimotor systems have relative simplicity and stereotyped neural structures (when compared to those of vertebrates), with few neurons generating complex behaviors. They are therefore better suited to developing analytical methods such as

✉ Fernando P. Santos
  fernandopasq@gmail.com; fernando.pasquini.santos@usp.br

[1] Faculty of Electrical Engineering, Federal University of Uberlândia, Av. João Naves de Ávila, 2160, Bloco 3N, Uberlândia 38408-100, MG, Brazil

[2] Signal Processing Laboratory, Department of Electrical Engineering, University of São Paulo, Av. Trabalhador Sãocarlense, 400, São Carlos 13566-590, SP, Brazil

[3] Biological Sciences, University of Southampton, Highfield Campus, Southampton S017 1BJ, UK

data acquisition and analysis techniques than vertebrates and in providing insights into the control of robots and prostheses (Buschmann et al. 2015; Kovač 2014; Vitanza et al. 2015). Recent studies have focused on the locust hind leg and the role of proprioception in the control of reflex movements. Using a Wiener-kernel method of analysis Kondoh et al. (1995) showed that the sensory neurons of a femoral chordotonal organ (FeCO), responsible for proprioceptive control about the 'knee' joint in the locust, encoded the position, velocity and acceleration of movements of the tibia about the femoro-tibial joint. Subsequently, Vidal-Gadea et al. (2010) modeled the responses of spiking local interneurons within the central nervous system using system identification with Wiener-kernel methods and cross-validation parameter estimation. While these methods provided improved estimates of responses over previous studies they were still subject to a number of limitations due to the nonlinear responses of the interneurons (Dewhirst et al. 2013). Improved methods using a Volterra model with complexity reduced by Laguerre basis functions were developed, and applied to a population of non-spiking local interneurones responsible for premotor control in the same neural networks. Recently, Meruelo et al. (2016) again improved this modelling by employing Artificial Neural Networks in system identification, while Endo et al. (2015) employed information theoretic approaches to understand interactions between neurons in the same neural network to predict connectivity patterns that correlated strongly with known morphological and physiological connectivity (Burrows 1996).

The use of information theory in understanding analogue synaptic signalling has received far less attention compared to its use on spike data. Part of that problem is due to a lack of identifiability of neurons within and between vertebrates, but also the non-stationarity of intracellular recordings, unlike spike data, that present a number of challenges (Dewhirst et al. 2013) such as the need for greater amounts of data for the estimation of probability distributions (Kaiser and Schreiber 2002; Pampu et al. 2013). The length of recordings needed to maintain stable recordings for analysis means that there is the potential for many factors to lead to DC offsets, and trends in the data caused by extrinsic factors, but also due to intrinsic non-stationary properties of the signal itself. In the latter case, several models have been proposed that rely on cyclostationarity and multiple repetitions of a recording (Wollstadt et al. 2014), or estimating different models separated by change-points (Grzegorczyk and Husmeier 2009).

In this study we consider the cause of the non-stationarity present in the signals as irrelevant to the model and associate it with experimental artifacts, based on the visual inspection of the signals, and the success of previous studies in finding consistent connections by considering only stationary parts under a Gaussian White Noise input signal (Dewhirst et al.

2013; Endo et al. 2015). Thus, we investigate the use of a Singular-Spectrum Analysis (SSA) method for removing non-stationarities from intracellular recordings as a preprocessing step, prior to transfer entropy estimation, to remove complex trends and discontinuities in the signal. Not only does this preprocessing step generate stationary signals that are a requirement for causality measures such as transfer entropy (Barnett and Seth 2011), but it also increases the availability of useable data. We then analyse these preprocessed signals from identified motor neurons and determine the effect of signal length on delayed transfer entropy measures. Finally, we determine the consistency of transfer entropy measures in identified neurons both within and between animals.

2 Materials & methods

2.1 Data acquisition

Data were previously collected by Newland and Kondoh (1997a, b) from adult male and female desert locusts (*Schistocerca gregaria* Forskål) that were immobilized ventral-side-uppermost in modeling clay, with their hind left leg fixed anterior surface uppermost. The FeCO was exposed by opening a small window in the cuticle of the distal femur and its apodeme exposed. This was the grasped by forceps mounted on a Ling shaker and driven with a 27 Hz band-limited Gaussian White Noise (GWN) signal as input to the neural circuits (see Newland and Kondoh 1997a, b for more details). The outputs, analogue synaptic potentials, were recorded intracellulary from the somata of motor neurons in the metathoracic ganglion (Fig. 1) with a sampling rate of 24 kHz. Hind leg motor neurons were identified as unique individuals based on the spatial location of their somata in the ganglion and their physiological properties (Burrows 1996).

2.2 Singular-spectrum analysis and preprocessing

To remove artifacts and complex non-stationary trends in the intracellular recordings of motor neurons unrelated to the stimulus input we used singular-spectrum analysis (SSA). SSA is an effective model-free method to remove complex trends in time-series and decomposes a data series into the sum of a small number of independent and interpretable components (Hassani 2007) and reconstructs it according to desired components (more details in Appendix A).

The SSA algorithm was applied to each intracellular signal recorded in the experiments and the signal was reconstructed without the component associated with the largest eigenvalue. This was based on Palus and Novotná (1998) who showed that SSA decomposes a time-series into orthogonal
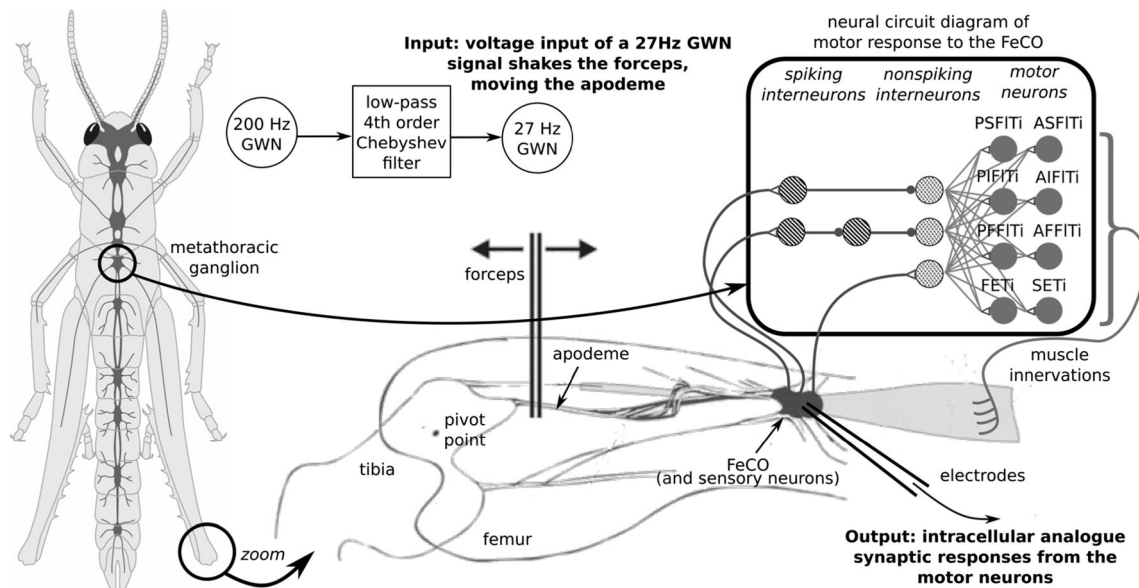
Fig. 1 Experimental setup for the collection of data from hind leg motor neurons controlling movements of the tibia about the knee joint. The input to the neural network was generated using a Gaussian White Noise (GWN) generator with a cut-off frequency of 27 Hz, and used to move forceps attached to the apodeme of the FeCO. The output of the neural networks were recorded using intracellular microelectrodes as synaptic potentials of motor neurons in the metathoracic ganglion

components (modes) with different dynamical properties, and that the eigenvalues related to slow modes (or trends) are much larger than eigenvalues of the modes related to higher frequencies. Thus, the largest eigenvalue can be regarded as being associated with complex trends and slow discontinuities (i.e., with low frequencies when compared to the higher ones present in the signal). The SSA-MTM Toolkit (Vautard et al. 1992) was then used with window length parameters of 2000 samples (83.3 ms), decomposing the signal into 64 principal components and reconstructing it with 63 (excluding the lowest oscillatory component).

2.3 Delayed transfer entropy measures

Recently the use of directed information transfer measures, such as Transfer Entropy and Conditional Transfer Entropy, have been applied to physiological data to determine network structures describing dependencies and independencies between regions of the brain or neurons (Wibral et al. 2014).

Given two time-series X and Y, transfer entropy (Schreiber 2000) is defined as the "amount of information that a past state of X contains about a future observation of a process Y, given the past state of Y", thus defined generically by (Wibral et al. 2014) as:

$$TE(X \rightarrow Y) = I(X^-, Y^+ \mid Y^-) \quad (3)$$

where X^- and Y^- are past states of processes X and Y. Schreiber (2000), by assuming a generalized Markov

property, proposed transfer entropy to be estimated according the following expression:

$$
\begin{aligned}
TE(X \rightarrow Y) &= I\left(y_{n+1}, x_n^{(l)} \middle| y_n^{(k)}\right) \quad (1) \\
&= \sum_{\substack{\forall x \in X \\ \forall y \in Y}} P\left(y_{n+1}, y_n^{(k)}, x_n^{(l)}\right) log \frac{P\left(y_{n+1} \middle| y_n^{(k)} x_n^l\right)}{P\left(y_{n+1} \middle| y_n^{(k)}\right)}
\end{aligned}
$$

where P are probability mass functions for processes X and Y with alphabets $\mathcal{X}$ and $\mathcal{Y}$. $y_n^{(k)}$ stands for k past states of Y and $x_n^{(l)}$ for l past states of X.

We used 32 even width bins for discretization, based on the mean data length close to 320,000 samples, and estimated probability mass functions through histograms. In addition, we fixed $k = 1$ and $l = 1$, under the supposition that the underlying system was Markovian (i.e. present states depend only on immediate past states), which may be a rough approximation, however it is what is possible given the data available. Standard practice would include searching for an appropriate embedding dimension such as through the Ragwitz criteria as pointed out by Wibral et al. (2014).

The immediate past state of Y also had to be determined since our experimental sampling rate (24 kHz) did not automatically correspond to it. We defined the delay of the immediate past, or embedding delay, as α, and employed the technique for delay embedding proposed by Kantz and Schreiber (2004). This delay was thus estimated following the practice of obtaining the first minimum found in the delay of the auto mutual information of the time-series (Kantz and

Schreiber 2004). The system could also be subsampled in order for $y_{n-\alpha}$ to correspond to y_{n-1} (i.e., the immediate past), however, this could also compromise the resolution of the time delay found between the two processes, as explained below. Wibral et al. (2013), however, argued recently that best practice is assured by setting $\alpha = 1$ in the experimental sampling, since it would better consider the influence of memory in the transfer entropy measures. This analysis, however, will be conducted in further experiments.

Transfer entropy is then used to find the time-delay between two variables in the complex system. These time-delays are obtained by considering the maximum peak of information transfer in a sweep of different delays between two signals (Silchenko et al. 2010; Wibral et al. 2013). Thus, with the assumptions above, the *delayed transfer entropy* is calculated as:

$$TE(X \rightarrow Y, \beta) = I\big(y_n, x_{n-\beta} | y_{n-\alpha}\big) \qquad (2)$$
$$= \sum_{\substack{\forall x \in X \\ \forall y \in Y}} p\big(y_n, y_{n-\alpha}, x_{n-\beta}\big) log \frac{p\big(y_n | y_{n-\alpha}, x_{n-\beta}\big)}{p\big(y_n | y_{n-\alpha}\big)}$$

and the time-delay between two processes X and Y obtained as $\delta = \arg \max_{\beta}(TE(X \rightarrow Y, \beta))$ (Pampu et al. 2013; see Wibral et al. 2013 for the formal proof).

Finally, it was also important to consider the effect of noise and finiteness of the data in these information measures, eliminating bias and evaluating the significance of these measures. A number of tools are available for bias correction, such as the KSG estimator or the Miller and Madow type correction (Wibral et al. 2014). However, for the purposes of statistical significance tests one usually generates surrogate data (Schreiber and Schmitz 2000), which represents, as best as possible, all the characteristics from the real process, but with no information transfer. Thus, a comparison can be made between the original signal and surrogate data. In the case of neurophysiological data, information transfer happens in phase synchronization (Yang et al. 2013), and thus Endo et al. (2015) proposed the generation of surrogate data with the Iterative Amplitude Adjusted Fourier Transform (AAFT) algorithm, which generated signals preserving the signal's power density spectrum but randomly shuffling its phase components (Venema et al. 2006). An alternative is simply shuffling the samples of the original time-series, as a way of destroying the temporal precedence structure (Wibral et al. 2014). Dolan and Spano (2001) showed, however, that this method preserves the same amplitudes and frequencies of samples, and thus may not provide too much variability for estimating probability distributions with limited data. Thus, in this study, we employed the AAFT algorithm due to its better ability to catch the bias due to limited data and, also, for its computational efficiency.

The values of delayed transfer entropy obtained, however, may also vary according to the signals recorded and the number of samples employed in their estimation (Ince et al. 2012). A debiasing and normalization procedure must therefore be applied to make these measures comparable across experiments. Gourevitch and Eggermont (2007) proposed that transfer entropy measures should be normalized by the difference between transfer entropy with the original data and the mean transfer entropy with surrogate data (i.e. a debiasing procedure) over the entropy of the actual value of the target variable given its past, $H(Y_n | Y_{n-\alpha})$, which is defined as

$$H(Y_n | Y_{n-\alpha}) = - \sum_{\substack{\forall x \in X \\ \forall y \in Y}} P(y_n, y_{n-\alpha}) \log \frac{P(y_n, y_{n-\alpha})}{P(y_{n-\alpha})} \qquad (3)$$

and therefore we obtain the normalized delayed transfer entropy (Gourevitch and Eggermont 2007):

$$\widehat{TE}(X \rightarrow Y, \beta) = \frac{TE(X \rightarrow Y, \beta) - TE(X_{\text{surrogate}} \rightarrow Y, \beta)}{H(Y_n | Y_{n-\alpha})} \in [0, 1] \qquad (4)$$

Delayed transfer entropy throughout the entire dataset was always evaluated between the input 27 Hz GWN displacement of the FeCO apodeme and the respective intracellular recording of synaptic responses from a motor neuron. From each of these pairs of data, 10 surrogate data series were generated to infer the noise level (the number was chosen according to feasibility given the computational time available). The complete process is shown in Fig. 2.[1]

2.4 Statistical analysis

To evaluate how well our method based on surrogate data was able to exclude spurious peaks found in the delayed transfer entropy measures, we use a statistical power test for obtaining the confidence level (Schreiber and Schmitz 2000). The test compares the TE statistic against that obtained from N surrogates, and rejects the null hypothesis of no directed relationship between source and target if the TE statistic is greater than all N surrogate measurements. The relationship between the number of surrogate data (N) employed and the probability of false rejection (α), corresponding to the level of significance (Therrien 1992), is given as $N = K/\alpha - 1$, where $K = 1$ for a one-sided test and $N = 10$ in our experiment. Thus, the estimated confidence level was close to 91% (i.e., the probability to correctly reject a spurious peak). This was limited due

---

[1] The code used in the analysis is publicly available at https://github.com/lablps/JCNS2017. Further information may be obtained by contacting the authors.
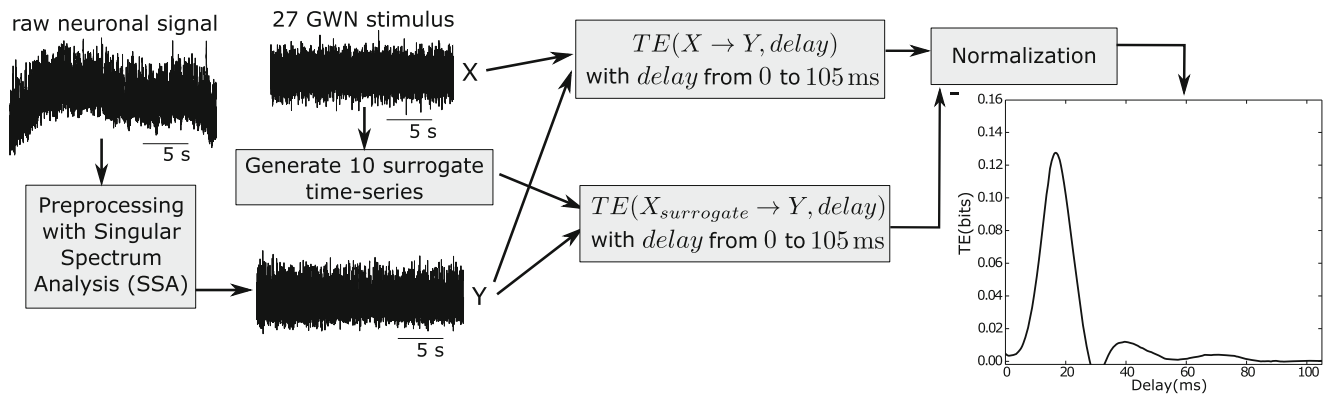
Fig. 2 Data preprocessing with SSA and information transfer measures applied to intracellular recordings of synaptic responses obtained from a hind leg motor neuron. Transfer entropy was applied to the 27 GWN stimulus (X) to motor neurons (Y) and from 10 surrogate time-series from the stimulus generated through the AAFT algorithm. The number of surrogates was chosen arbitrarily, considering that an increase considerably impacts the time of execution. Normalization was applied according to Eq. (4)

to computational cost, which was associated with the fact the we performed a direct estimation of transfer entropy from histograms (as outlined in Section 2.3), the length of the data files and the repetitions during the sweeping of time delays for the original and surrogate data. The additional computation of surrogate data and transfer entropy had a large impact on data set analysis and would have moved the analysis from a scale of weeks to months if a confidence level of 97% ($N = 30$) were to be used.

3 Results

3.1 Pre-processing

To determine the effectiveness of pre-processing at removing artifacts and non-stationarities from intracellular recordings we applied SSA to intracellular recordings in which the FeCO was stimulated with a 27 Hz band limited GWN signal while the synaptic responses of different identified leg motor neurons were recorded intracellularly from their somata. In particular, we analysed recordings of motor neurons that were excluded from previous studies (Dewhirst et al. 2013; Newland and Kondoh 1997a, b) due to their non-stationarities, including those showing simple trends (Fig. 3a) to those showing abrupt changes (Fig. 3b). In total we analysed 216 signals from motor neurons ranging in length from 17.8 s to 123.7 s (41.43 ± 15.94 s, mean $\pm$ SEM). Based on a Wald-Wolfowitz test of stationarity (Grazzini 2012) we found that 36.6% of the data was stationary before SSA pre-processing, however following pre-processing using SSA 95.8% of the data was stationary and useable for analysis of delayed transfer entropy. Unstable data was removed from subsequent analyses.

3.2 The impact of signal length on transfer entropy measures

To determine the effect of data length on delayed transfer entropy measures of the synaptic responses of identified neurons we analysed the pre-processsed intracellular recordings from a posterior slow flexor tibiae (PSFlTi) motor neuron (Fig. 4). An analysis of delayed transfer entropy revealed 2 distinct peaks in association between the synaptic response and the GWN input to the FeCO. The original recording of this motor neuron contained 1.2 M samples (labeled 12 on Fig. 4). We then cut the data into 100 k samples so that trace 1 was 100 k in length, trace 2 was 200 k in length, trace 3 300 k in length and so on up to trace 12 containing 1.2 M samples (labeled 1–12 in Fig. 4). Absolute values of delayed transfer entropy were then calculated, however, these could include false positive results, and thus the significance of the measures were tested against surrogate data.for spurious peak association which is represented by the noise levels in Fig. 4. Noise levels from surrogate data were determined for each independent recording, and in this case the noise levels determined by the surrogate data are shown only for traces 1, 2 and 12 for clarity. With reducing signal length the noise levels increased markedly (compare surrogate data traces in red in traces 1 and 12 in Fig. 4).

DTE was applied and the behaviour of the data in three different identified motor neurons, each from a different animal, and with three different recording lengths were compared (Fig. 5). For example, recordings from FETi with three different recording lengths are shown in the top row of Fig. 5, three examples of the PSFlTi from a different animal with three recording lengths are shown in the middle row, while three recordings of the Anterior Intermediate Flexor Tibiae (AIFlTi) motor neuron from a different animal are shown in the lower row. Results show a general increase in the value of delayed transfer entropy with signal length, leading to a saturation. For
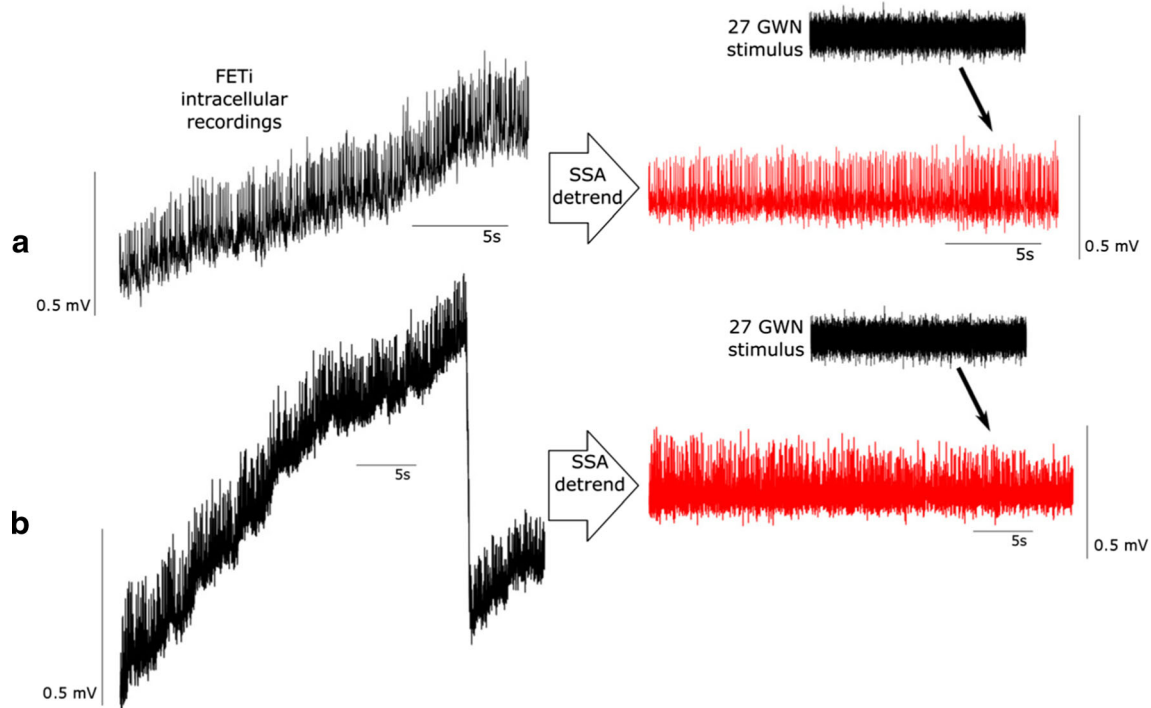
Fig. 3 Examples of intracellular recordings from the somata of the fast extensor tibiae motor neuron. **a** An example of a recorded signal from the fast extensor tibiae (FETi) showing a continuous drift in the membrane potential of the motor neuron. **b** An example of a recording of FETi from a different animal showing both continuous trends and abrupt changes in membrane potential. Following SSA pre-processing both signals displayed stationarity data and were subsequently analysed

example, analysis of synaptic responses in FETi revealed a single peak in DTE. With 171,513 samples (7.34 s trace length) the difference between the peak in DTE and the mean DTE of the surrogate data was 0.412 bits. With 343,027

Fig. 4 Effect of signal length on transfer entropy. A recording from a posterior slow flexor tibiae (PSFlTi) motor neuron was cut into 100 k samples from 100 k (trace 1) to 1.2 M samples (trace 12) and labeled 1 to 12 (*blue traces*). Analysis of transfer entropy revealed two distinct peaks. Surrogate data (*red traces*), representing the noise level, was used as a test of significance of the peaks in transfer entropy. Both the significance and the noise level decreased with increasing samples due to the use of 32 bins for discretization

samples (14.29 s trace length), approximately double the signal length, the difference increased to 0.543 bits while with 686,094 samples (28.58 s trace length) the difference rose to 0.547 bits (thus, a saturation occurred). Similarly, for the PSFlTi motor neuron a recording with 172,513 samples revealed two distinct peaks in DTE with the difference between DTE in the first peak and the mean DTE of the surrogate data of 0.267 bits. With 343,027 samples, the difference increased to 0.342 bits while for 860,547 samples the difference rose to 0.336 bits. Finally, a similar relationship existed for the AIFlTi motor neuron (third row in Fig. 5) in which a recording with 180,200 samples, revealed two distinct peaks in DTE. The difference between DTE in the first peak and the mean DTE of the surrogate data was 0.246 bits. With 348,521 samples, the difference increased to 0.276 bits, while for 757,043 samples the difference rose to 0.300 bits. Also, for each motor neuron, the longer the data length the lower the mean noise level and variation.
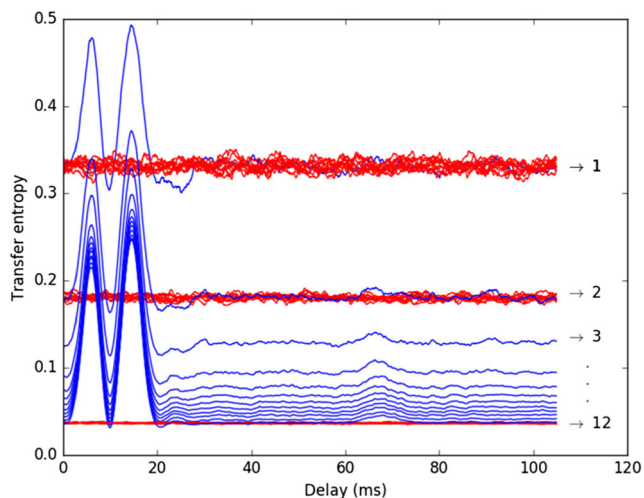
3.3 Consistency of delayed transfer measures

To establish delayed transfer entropy (DTE) as a useful tool to model functional connectivity based on intracellular recording of synaptic responses in neural networks it was important to establish that DTE estimates from given identified neurons were consistent from the same neuron in a single animal over the time course of a single experiment, over
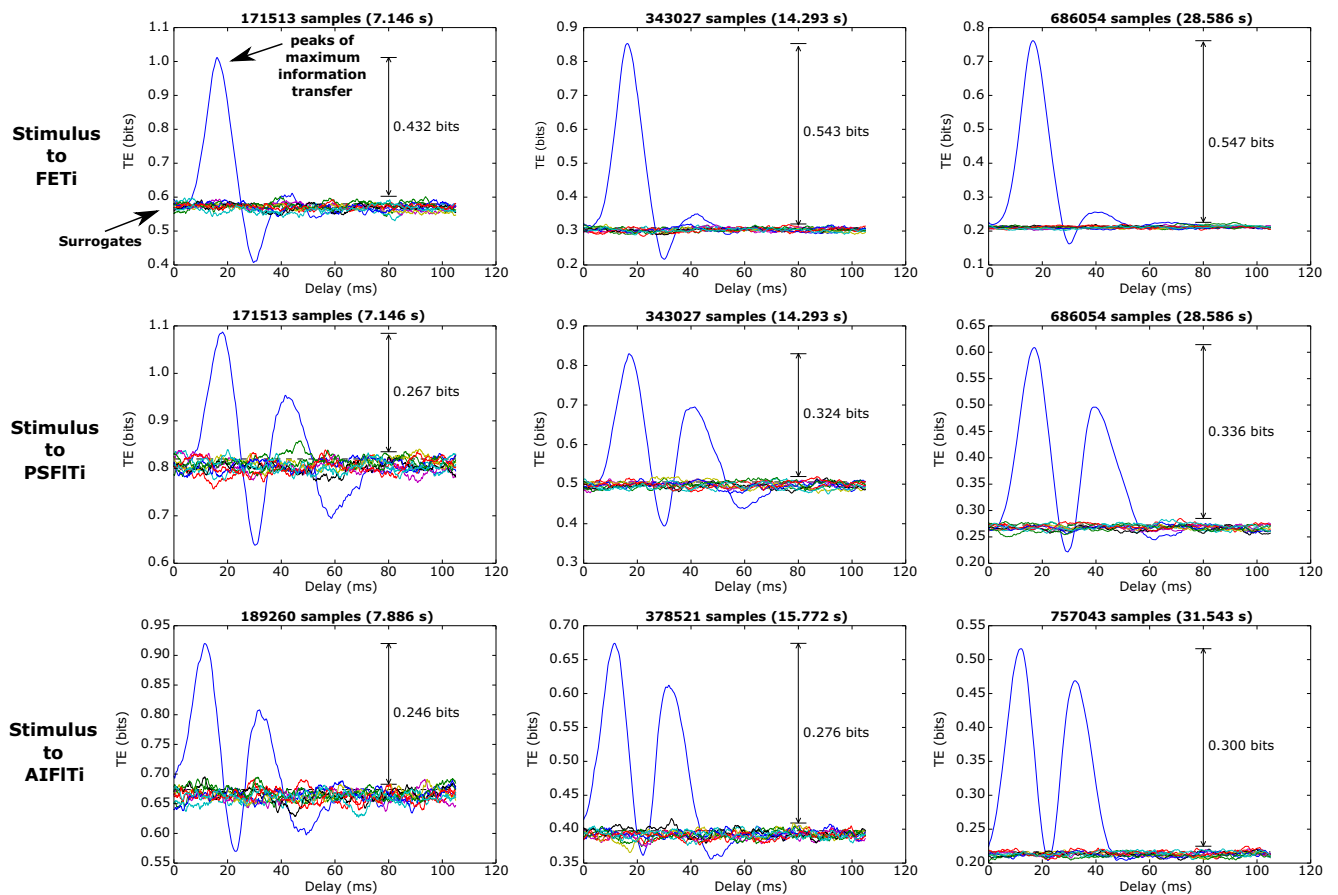
Fig. 5 Effect of recording length on DTE. DTEs were calculated between the input GWN to the FeCO and motor neuron synaptic response. Top traces, DTE measures in FETi for three different recording lengths (sample sizes). Middle traces, DTE measures from the PSFlTi motor neuron for three recording lengths, and bottom traces, DTE measures in the AIFlTi motor neuron for three recording lengths. In each identified neuron the significance of DTE measures increased with signal length (sample size) that saturated

multiple experiments from the same identified neuron in the same animal, and finally between identified neurons in different animals.

3.3.1 Consistency of DTE measures from the same neuron over time within a single experiment

To test whether delays in information transfer occurred during the time course of an experiment form an individual motor neuron (and thus the SSA detrending method sufficient to obtain a stationary model), we tested consistency of DTE within a recording. We took long recordings from specific neurons following SSA pre-processing, divided them into three segments and evaluated the DTE in each segment. For example we, compared three equally sized parts of an intracellular recording of FETi of approximately 1.2 M samples (50 s) and found that it showed a single distinct peak with a mean delay 15.97 ± 0.41 ms (Fig. 6) over the three sections of data, implying no significant variation in peak times throughout the duration of the recording. Based on these DTE

measurements we evaluated the normalized standard deviation and found that the percentage of peaks with a normalized standard deviation of less than 5 % was 88%, while at 10 % it was 98%.

3.3.2 Consistency of DTE measures from the same neuron between repeated experiments in the same and different animals

To determine the consistency of DTE measures of an identified motor neuron between six repetitions of the same experiment at 5 min intervals within the same animal we used data in which the FeCO apodeme was stimulated with a 27 Hz band-limited GWN for approximately 45 s while the evoked synaptic responses were recorded intracellularly from FETi. DTE measures in each experiment revealed responses with similar peak times of 15.49 ± 0.49 ms (mean $\pm$ SEM) indicating consistency over time in the same animal (Fig. 7a).

To determine the consistency of DTE measures of an identified motor neuron in different animals we again compared
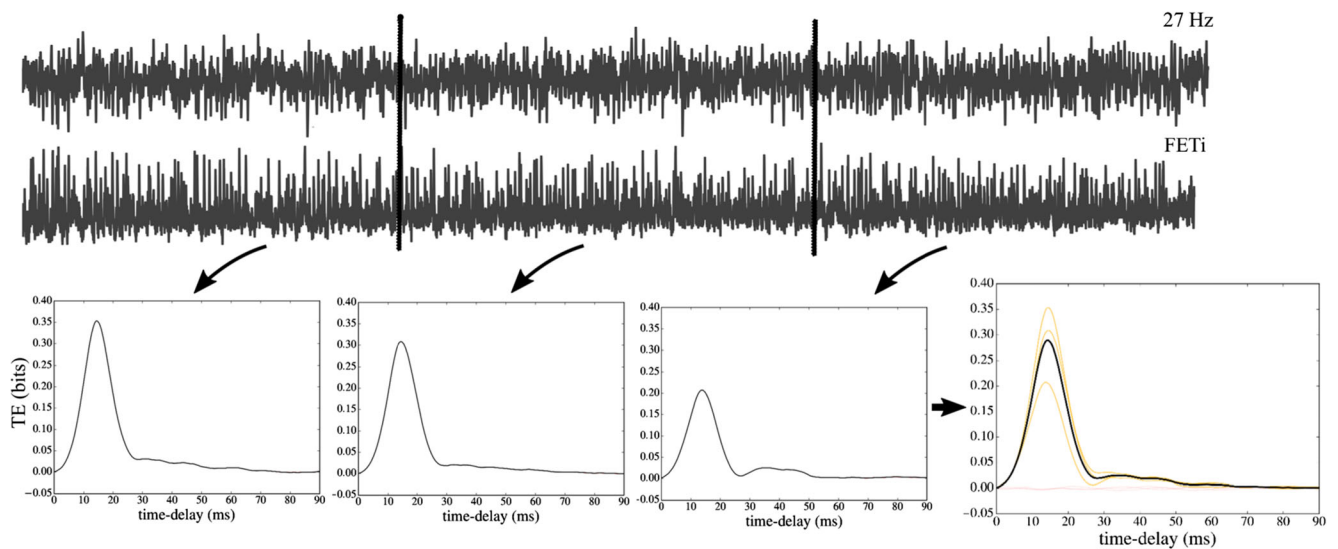
Fig. 6 Consistency of DTE measures over time within a single experiment. Comparison of non-normalized DTE measures over three segments (of approximately 16.6 s) of a time-series recorded from a FETi motor neuron showing consistent peak times. The mean peak in delay was 15.97 ± 0.41 ms, indicating little variation along the signal

different recordings with the longest possible lengths greater than 45 s. Results showed that the patterns of DTE were similar between the same identified neuron in different animals, which can be seen clearly when the DTE measures are superimposed (Fig. 7b). The mean time to peak of FETi in eight different animals was 16.48 ± 1.01 ms (mean ± SEM). Experiments from different animals with different lengths, and therefore different noise levels, revealed consistent DTE patterns from the same motor neuron between animals.

4 Discussion

Analysis of transfer entropy is increasingly becoming a key tool for understanding connectivity and information transfer in neural networks (Gourevitch and Eggermont 2007; Faes and Porta 2014. Wibral et al. 2014; Schroeder et al. 2016). Here we have developed methods to preprocess synaptic

responses recorded intracellularly from identified neurons in a proprioceptive network to recover and enhance stationarity for analysis, and take advantage of the identifiability of individual motor neurons in the locust to test the consistency and repeatability of transfer entropy estimates both within and between animals. We showed that preprocessing using Singular Spectrum Analysis was effective at generating longer stationary time series that can be used in analysis of transfer entropy, and that transfer entropy estimates from synaptic signals were highly dependent on sample size/recording length. We were then able to show that transfer entropy estimates were consistent over the time course of a single experiment for an identified neuron in an individual animal, were consistent and repeatable between multiple experiments from the same animal, and also consistent for the same neuron between animals. This is the first time that the accuracy and repeatability of transfer entropy has been tested directly on the synaptic responses of identifiable neurons.

Fig. 7 Consistency of DTE within and between animals. **a** DTE from 6 separate recordings from FETi in the same animal. The solid black line indicates the mean DTE. **b** DTE estimates from a single recording from FETi in eight different animals. The solid black line indicates the mean DTE, and the coloured lines the DTE from each animal
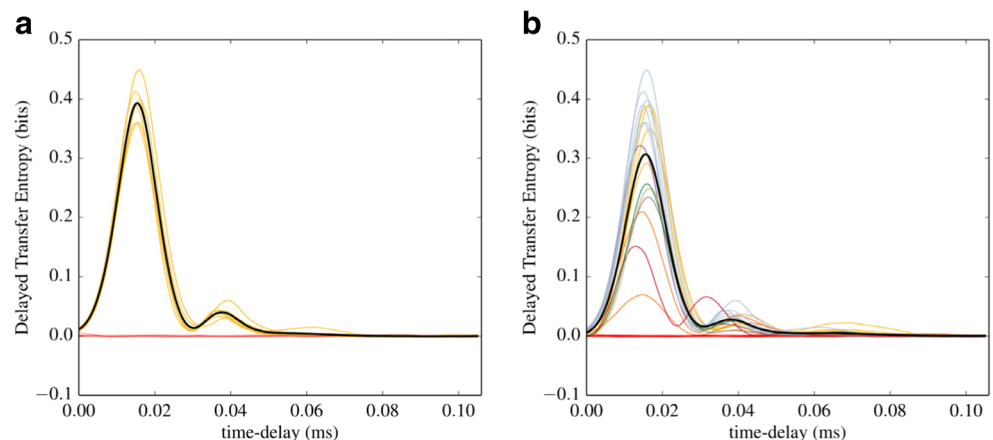
4.1 Computational analysis and preprocessing

We have used an information theoretic approach to understanding the transfer of information in a well-studied neural network that produces limb reflex movements in locusts (Burrows 1996). Since Schreiber (2000) introduced the general concept of transfer entropy, the technique has been applied successfully to many different systems and different types of data, in particular spiking neurophysiological data, due to its characteristics of asymmetry and coupling inference (Knoblauch and Sommer 2016; Orlandi et al. 2014). One of the advantages of transfer entropy is that it is a model free approach that makes no assumptions about the models that underlie the interactions between processes (Faes and Porta 2014). Hlaváčková-Schindler et al. (2007) and Lee et al. (2012) point out that the estimation of transfer entropy from time series data, such as the synaptic responses of FETi evoked by FeCO stimulation, is complicated by a number of practical problems, including that of estimating probability density functions underlying transfer entropy computation on restricted datasets whose lengths may be limited by experimental constraints and/or due to non-stationarity. Here we have used SSA preprocessing to overcome some of these problems.

In comparison to delayed mutual information (Endo et al. 2015), transfer entropy conditions the entropy between two processes on the past states of the target process and thus excludes some of the memory effects by capturing the synergy between the source process and the past states of the target process (Marinazzo et al. 2014). It is important to note however, that a proper embedding dimension of the time-series is needed to completely differentiate information flow from memory. Here we did not achieve this given the histogram approach employed that required the assumption of a first order Markovian system ($k = l = 1$) due to the high demands of data.

Nevertheless, a comparison between delayed mutual information measures and the delayed transfer entropy measure developed here already reveals new information about the system studied. For example, a comparison between measures of delayed mutual information (Fig. 8a) and delayed transfer entropy (Fig. 8b) applied to the same recording of a PFFlTi motor neuron reveal that mutual information may fail to find definite peaks and continue to have significant values (over the surrogate level) with higher time delays. This could be interpreted as a memory effect resulting from not conditioning on the past of the target variable. Moreover, Kaiser and Schreiber (2002) showed that transfer entropy is an asymmetrical measure (which is not the case with mutual information) and thus can better represent the directionality of information transfer.

We have tested a preprocessing method to increase the length of useable data from intracellular recordings of identified motor neurons. Analysis of data with spike responses is often carried out using spike times of inter-spike intervals (Nawrot 2010), however, this was clearly impossible with synaptic responses and thus we proceeded to a detrending method. We also chose not to filter the intracellular signals with high-pass filters, such as those discussed by Barnett and Seth (2011), as this method requires determination of parameters such as cut-off frequency, among others, which can be highly arbitrary and can change from signal to signal. Moreover, a study by Florin et al. (2010) suggested that a simple filtering of neural data is prone to disturbing the ordering of the data, thus hindering the use of Granger causality measures (which is transfer entropy with the assumption of Gaussian processes (Barnett et al. 2009). Barnett and Seth (2011) explored this issue further and concluded that although Granger causality measures remain invariant under the application of invertible filters, in practice some changes may be present due to the increase of model order due to filtering.
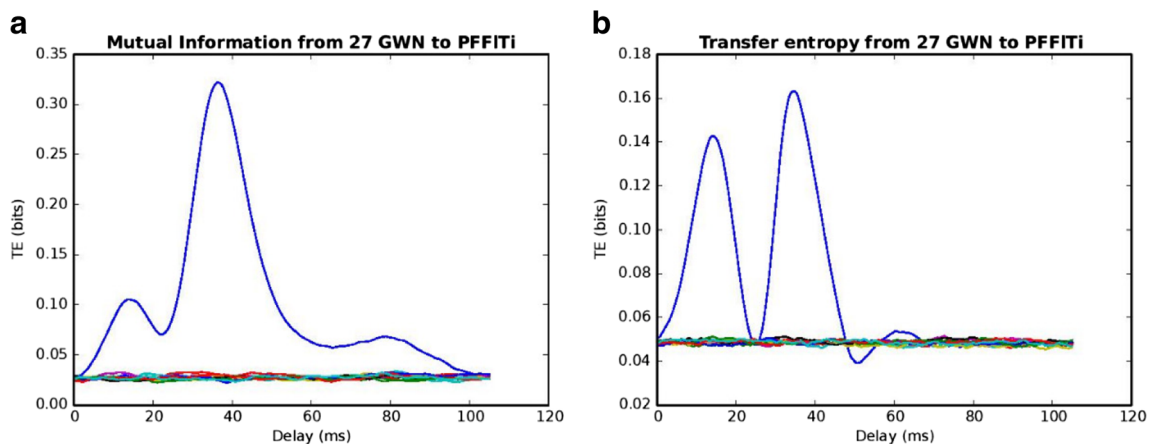

Fig. 8 Difference between delayed mutual information (**a**) and delayed transfer entropy (**b**) applied to the same recording of a PFFlTi motor neuron. Transfer entropy revealed clearly defined peaks of information transfer and also eliminated the significant values at higher time-delays found with the delayed mutual information values

Since our model order was low there was a risk of missing or spurious causality measures even if the filtering was applied for removing non-stationarities.

By applying SSA as a preprocessing step to remove trends in data, the number of samples available for information transfer measures increased markedly compared to previous studies (Dewhirst et al. 2013; Endo et al. 2015) that analysed small stationary segments in the recorded time-series. This was only possible once it was clear that the trends represented extrinsic factors imposed on the signal by the experimental setup, and not reflecting characteristics of the neural response to be described in the model. This was also assured by the consistency test throughout the duration of an experiment presented in section 3.3.1, indicating no significant variation in the peak delay times throughout an experiment.

A common feature of neural circuits, and individual neurons, is that they often adapt to repetitive or constant stimulation (Benda et al. 2005; Prescott and Sejnowski 2008). This intrinsic adaptation provides many functions including facilitating stable limb control (Kittmann 1997), coincidence detection (Cook et al. 2003) and separating signals of different time scales (Benda et al. 2005). Adaptation to repetitive stimulation over a time scale of seconds has been shown to occur in the same locust local circuits we study here, at the sensory (Newland 1991), interneuron (Angarita-Jaimes et al. 2012; Vidal-Gadea et al. 2010) and motor neuron (Field and Burrows 1982) levels. Similar patterns of adaptation have also been shown in limb control networks in stick insects (Bässler 1993) and in proprioceptors in crabs (Gamble and DiCaprio 2003). Dewhirst et al. (2013), however, showed that key system dynamics remain relatively unchanged during repetitive stimulation while output amplitude adaptation occurs. Moreover, much of the adaptation occurs within the first few seconds of stimulus input which means that there are generally relatively long stationary periods from which data can be analysed (Kondoh et al. 1995). Here we find that DTE measure were consistent throughout a single experiment from a given identified motor neuron suggesting that information transfer delays remain invariant irrespective of any adaptation in amplitude of responses.

To evaluate parameters like entropy, mutual information and transfer entropy large data sets are required with at least wide sense stationarity properties (Wibral et al. 2014). Each of these measures is estimated based on histogram algorithms (two-dimensional for mutual information and three-dimensional for transfer entropy) and the greater the length of the data the better the estimates, and better models inferred. In addition, the need for larger datasets grows exponentially when analysis moves from entropy estimation to transfer entropy estimation (Wibral et al. 2014). For analyses of neural activity, whether in vertebrates or in invertebrates, experiments require animal use, are often time consuming and expensive and difficult to prepare. An ability to use all data to recover information is therefore a necessity. Pre-processing algorithms therefore represent an important step towards increasing the amount of useable data from experiments.

4.2 Connectivity in local circuits

The patterns of connections of FeCO afferents and central neurons, with the exception of FETi are well known. For example, FeCO stimulation has previously been shown to have an effect on FETi, in parallel with SETi (Meruelo et al. 2016; Dewhirst et al. 2013; Field and Burrows 1982) by evoking depolarization during flexion of the tibia, typical of a negative feedback reflex. In common with SETi, FETi shows position dependent responses during FeCO stimulation, however FETi has a greater dependence on velocity (Field and Burrows 1982). Burrows (1987) showed that flexor motor neurons appear to receive monosynaptic input from FeCO afferents, as do spiking local interneurons of a population with somata at the ventral midline of the metathoracic ganglion (Burrows 1988). Burrows et al. (1988) also showed that some FeCO afferents made monosynaptic depolarizing synaptic connections with nonspiking interneurons in parallel with flexor motor neurones, and with a central latency of 1.5 ms. Finally, Burrows (1988) found that inhibition in nonspiking interneurons during FeCO was the result of indirect GABAergic inputs from spiking local interneurons (Watson and Burrows 1987). Despite the considerable knowledge we have of the patterns of connections between FeCO afferents and leg motor neurons we know little of the details of the synaptic connections between the FeCO afferents and FETi.

Endo et al. (2015) analysed the synaptic responses of nonspiking interneurons in response to FeCO stimulation and found three distinct time delays in delayed mutual information (DMI) between mechanical excitation of the FeCO and the neuronal responses. One group of nonspiking interneurons had mean delays of DMI of 14.2 ± 0.4 ms (mean $\pm$ SEM), a second group exhibited peaks of DMI at 25.7 ± 1.3 ms while a third group had two pronounced peaks of DMI at 31.8 ± 0.9 ms and 45.3 ± 1.5 ms. Endo et al. (2015) argued that the times to peak DMI were related to known physiological pathways (Burrows 1996) and that the shortest time delays were most likely due to direct monosynaptic excitatory connections between FeCO sensory afferents on the interneurons (Burrows et al. 1988). They also analysed the DMI in spiking local interneurons and found that they could be divided into two groups based on time to peak of DMI, and concluded that those with the shortest time delays were again likely to be due to monosynaptic inputs from sensory neurones that are known to be present (Burrows 1988). Results from our analyses of DTE in FETi here show consistent estimates from repeated experiments within the same and different animals of delay lengths similar to known monosynaptic inputs to spiking and nonspiking interneurons and flexor

tibiae motor neurons (Burrows 1987, 1988), and therefore suggest that the major excitatory input to FETi during resistance reflexes mediated by the FeCO is via excitatory monosynaptic input. Thus our analysis and models predict that there is likely to be functional connectivity that has yet to be revealed using more traditional physiological and morphological analyses and highlight the value of computational modelling in understanding connectivity in neural networks.

In this study we have developed methods and tested consistency of delayed transfer entropy measures from recordings of synaptic activity recorded from identified motor neurons. The aim now is to use these techniques to understand how information is transferred between every layer in local circuits and between synaptic input and spike output within an individual neuron. The neural circuits underlying local movements of the leg of the locust therefore represent an ideal system in which to address fundamental properties of information transfer in neural circuits.

Compliance with ethical standards

Conflict of interest The authors declare that they have no conflict of interest.

Appendix A: Singular spectrum analysis

The SSA algorithm is described as follows (Golyandina and Zhigljavsky 2013): consider a time-series $Z_T = (z_1, \ldots, z_T)$. The embedding matrix of Z is obtained as:

$$\boldsymbol{Z} = \left(z_{ij}\right)_{i,j=1}^{L,K} = \begin{pmatrix} z_1 & z_2 & z_3 & \ldots & z_K \\ z_2 & z_3 & z_4 & \ldots & z_{K+1} \\ \vdots & \vdots & \vdots & \vdots & \vdots \\ z_L & z_{L+1} & z_{L+2} & \ldots & z_T \end{pmatrix} \quad (5)$$

where $K = T - L + 1$ and L are window lengths considered for calculation ($L \leq T/2$). It is also important to note that $\boldsymbol{Z}$ is a Hankel matrix and has equal elements on the anti-diagonals. A singular value decomposition (SVD) value is be applied to the matrix $\boldsymbol{ZZ'}$, representing it as a sum of rank-one bi-orthogonal elementary matrices. We then denote $\lambda_1, \lambda_2, \ldots, \lambda_L$ is as the eigenvalues of $\boldsymbol{ZZ'}$ in decreasing order of magnitude $\lambda_1 \geq \ldots \geq \lambda_L \geq 0$ and $\boldsymbol{P} = (P_1, P_2, \ldots, P_L)$ is the orthonormal system of the eigenvectors of $\boldsymbol{ZZ'}$ corresponding to these eigenvalues (Golyandina and Zhigljavsky 2013). We also define d as $d = \max(i, \text{such that } \lambda_i > 0) = \text{rank } \boldsymbol{Z}$ (in real data, we

usually have $d = \min \{L, K\}$).

The principal components (PCs) V_i ($i = 1, \ldots, d$) of the embedding matrix are then obtained by $V_i = \boldsymbol{Z}' P_i / \sqrt{\lambda_i}$, and thus the trajectory matrix can be written as $\boldsymbol{Z} = \boldsymbol{Z}_1 + \boldsymbol{Z}_2 + \boldsymbol{Z}_3 + \ldots + \boldsymbol{Z}_d$, where $\boldsymbol{Z}_i = \sqrt{\lambda_i} P_i V_i'$ ($i = 1, \ldots, d$). These matrices have rank 1, and therefore are called *elementary matrices* (Hassani 2007).

The signal, then, can be reconstructed by selecting PCs according to their desired properties and then projecting them back to the original coordinates of the time-series. This is done by selecting and partitioning the indices $i = 1, \ldots, d$ into disjoint subsets $I_1, I_2, \ldots, I_m$. Then, for a given subset $I = \{i_1, i_2, \ldots, i_Q\}$ the corresponding resultant matrix $\boldsymbol{Z}_I$ is defined as $\boldsymbol{Z}_I = \boldsymbol{Z}_{i_1} + \boldsymbol{Z}_{i_2} + \ldots + \boldsymbol{Z}_{i_Q}$. This also leads to the SVD decomposition being represented as $\boldsymbol{Z} = \boldsymbol{Z}_{I_1} + \boldsymbol{Z}_{I_2} + \ldots + \boldsymbol{Z}_{I_m}$.

Diagonal averaging is then applied to a matrix X_{I_k} producing the reconstructed time-series $\tilde{Z}^{(k)} = \left(\tilde{z}_1^{(k)}, \tilde{z}_2^{(k)}, \ldots, \tilde{z}_T^{(k)}\right)$. In this way, the original series is decomposed into a sum of m reconstructed subseries:

$$z_n = \sum_{k=1}^{m} \tilde{z}_n^{(k)}, (n = 1, 2, \ldots, T) \quad (6)$$

With this, SSA can be used as a tool for time-series smoothing, extraction of trends and extraction of oscillatory components (Golyandina and Zhigljavsky 2013).

References

Angarita-Jaimes, N., Dewhirst, O. P., Simpson, D. M., Kondoh, Y., Allen, R., & Newland, P. L. (2012). The dynamics of analogue signaling in local networks controlling limb movement. *European Journal of Neuroscience, 36*(9), 3269–3282.

Barnett, L., & Seth, A. K. (2011). Behaviour of Granger causality under filtering: theoretical invariance and practical application. *Journal of Neuroscience Methods, 201*(2), 404–419.

Barnett, L., Barrett, A. B., & Seth, A. K. (2009). Granger causality and transfer entropy are equivalent for Gaussian variables. *Physical Review Letters, 103*(23), 238701.

Bässler, U. (1993). The femur-tibia control system of stick insects—a model system for the study of the neural basis of joint control. *Brain Research Reviews, 18*(2), 207–226.

Benda, J., Longtin, A., & Maler, L. (2005). Spike-frequency adaptation separates transient communication signals from background oscillations. *Journal of Neuroscience, 25*(9), 2312–2321.

Burrows, M. (1987). Parallel processing of proprioceptive signals by spiking local interneurons and motor neurons in the locust. *Journal of Neuroscience, 7*(4), 1064–1080.

Burrows, M. (1988). Responses of spiking local interneurones in the locust to proprioceptive signals from the femoral chordotonal organ. *Journal of Comparative Physiology A, 164*(2), 207–217.

Burrows, M. (1996). *The Neurobiology of an Insect Brain*. Oxford: Oxford University Press.

Buschmann, T., Ewald, A., von Twickel, A., & Büschges, A. (2015). Controlling legs for locomotion—Insights from robotics and neurobiology. *Bioinspiration & Biomimetics, 10*(4), 041001.

Cook, D. L., Schwindt, P. C., Grande, L. A., & Spain, W. J. (2003). Synaptic depression in the localization of sound. *Nature, 421*(6918), 66–70.

Dewhirst, O. P., Angarita-Jaimes, N., Simpson, D. M., Allen, R., & Newland, P. L. (2013). A system identification analysis of neural adaptation dynamics and nonlinear responses in the local reflex control of locust hind limbs. *Journal of Computational Neuroscience, 34*(1), 39–58.

Dolan, K. T., & Spano, M. L. (2001). Surrogate for nonlinear time series analysis. *Physical Review E, 64*(4), 046128.

Ebeling, W. (2002). Entropies and predictability of nonlinear processes and time series. In *International Conference on Computational Science* (pp. 1209–1217). Berlin Heidelberg: Springer.

Endo, W., Santos, F. P., Simpson, D., Maciel, C. D., & Newland, P. L. (2015). Delayed mutual information infers patterns of synaptic connectivity in a proprioceptive neural network. *Journal of Computational Neuroscience, 38*(2), 427–438.

Faes, L., & Porta, A. (2014). Conditional entropy-based evaluation of information dynamics in physiological systems. In *Directed information measures in neuroscience* (pp. 61–86). Berlin Heidelberg: Springer.

Field, L. H., & Burrows, M. (1982). Reflex effects of the femoral chordotonal organ upon leg motor neurones of the locust. *Journal of Experimental Biology, 101*(1), 265–285.

Florin, E., Gross, J., Pfeifer, J., Fink, G. R., & Timmermann, L. (2010). The effect of filtering on Granger causality based multivariate causality measures. *NeuroImage, 50*(2), 577–588.

Gamble, E. R., & DiCaprio, R. A. (2003). Nonspiking and spiking proprioceptors in the crab: white noise analysis of spiking CB-chordotonal organ afferents. *Journal of Neurophysiology, 89*(4), 1815–1825.

Golyandina, N., & Zhigljavsky, A. (2013). *Singular Spectrum Analysis for time series*. Berlin Heidelberg: Springer-Verlag. http://www.springer.com/br/book/9783642349126.

Gourevitch, B., & Eggermont, J. J. (2007). Evaluating information transfer between auditory cortical neurons. *Journal of Neurophysiology, 97*(3), 2533–2543.

Grazzini, J. (2012). Analysis of the emergent properties: stationarity and ergodicity. *Journal of Artificial Societies and Social Simulation, 15*(2), 7.

Grzegorczyk, M., & Husmeier, D. (2009). Non-stationary continuous dynamic Bayesian networks. *Advances in Neural Information Processing Systems*, 682–690.

Hassani, H. (2007). Singular spectrum analysis: methodology and comparison. *Journal of Data Science, 5*(2), 239–257.

Hlaváčková-Schindler, K., Paluš, M., Vejmelka, M., & Bhattacharya, J. (2007). Causality detection based on information-theoretic approaches in time series analysis. *Physics Reports, 441*(1), 1–46.

Ince, R. A., Mazzoni, A., Bartels, A., Logothetis, N. K., & Panzeri, S. (2012). A novel test to determine the signi cancer of neural selectivity to single and multiple potentially correlated stimulus features. *Journal of Neuroscience Methods, 210*(1), 49–65.

Kaiser, A., & Schreiber, T. (2002). Information transfer in continuous processes. *Physica D: Nonlinear Phenomena, 166*(1), 43–62.

Kantz, H., & Schreiber, T. (2004). *Nonlinear time series analysis*. New York: Cambridge University Press. http://dl.acm.org/citation.cfm?id=289372.

Kittmann, R. (1997). Neural mechanisms of adaptive gain control in a joint control loop: muscle force and motoneuronal activity. *Journal of Experimental Biology, 200*(9), 1383–1402.

Knoblauch, A., & Sommer, F. T. (2016). Structural plasticity, effectual connectivity, and memory in cortex. *Frontiers in Neuroanatomy, 10*, 63.

Kondoh, Y., Okuma, J., & Newland, P. L. (1995). Dynamics of neurons controlling movements of a locust hind leg: Wiener kernel analysis of the responses of proprioceptive afferents. *Journal of Neurophysiology, 73*(5), 1829–1842.

Kovač, M. (2014). The bioinspiration design paradigm: A perspective for soft robotics. *Soft Robotics, 1*(1), 28–37.

Lee, J., Nemati, S., Silva, I., Edwards, B. A., Butler, J. P., & Malhotra, A. (2012). Transfer entropy estimation and directional coupling change detection in biomedical time series. *Biomedical Engineering Online, 11*(1), 19.

Meruelo, A. C., Simpson, D. M., Veres, S. M., & Newland, P. L. (2016). Improved system identification using artificial neural networks and analysis of individual differences in responses of an identified neuron. *Neural Networks, 75*, 56–65.

Nawrot, M. P. (2010). Analysis and interpretation of interval and count variability in neural spike trains. In *Analysis of parallel spike trains* (pp. 37–58). Boston: Springer. https://link.springer.com/chapter/10.1007%2F978-1-4419-5675-0_3.

Newland, P. L. (1991). Morphology and somatotopic organisation of the central projections of afferents from tactile hairs on the hind leg of the locust. *Journal of Comparative Neurology, 312*(4), 493–508.

Newland, P. L., & Kondoh, Y. (1997a). Dynamics of neurons controlling movements of a locust hind leg II. Flexor tibiae motor neurons. *Journal of Neurophysiology, 77*(4), 1731–1746.

Newland, P. L., & Kondoh, Y. (1997b). Dynamics of neurons controlling movements of a locust hind leg III. Extensor tibiae motor neurons. *Journal of Neurophysiology, 77*(6), 3297–3310.

Orlandi, J. G., Stetter, O., Soriano, J., Geisel, T., & Battaglia, D. (2014). Transfer entropy reconstruction and labeling of neuronal connections from simulated calcium imaging. *PloS One, 9*(6), e98842.

Palus, M., & Novotná, D. (1998). Detecting modes with nontrivial dynamics embedded in colored noise: Enhanced Monte Carlo SSA and the case of climate oscillations. *Physics Letters A, 248*(2), 191–202.

Pampu, N. C., Vicente, R., Muresan, R. C., Priesemann, V., Siebenhuhner, F., & Wibral, M. (2013, July). Transfer entropy as a tool for reconstructing interaction delays in neural signals. In *Signals, Circuits and Systems (ISSCS), 2013 International Symposium on* (pp. 1–4). IEEE.

Prescott, S. A., & Sejnowski, T. J. (2008). Spike-rate coding and spike-time coding are affected oppositely by different adaptation mechanisms. *Journal of Neuroscience, 28*(50), 13649–13661.

Schreiber, T. (2000). Measuring information transfer. *Physical Review Letters, 85*(2), 461.

Schreiber, T., & Schmitz, A. (2000). Surrogate time series. *Physica D: Nonlinear Phenomena, 142*(3), 346–382.

Schroeder, K. E., Irwin, Z. T., Gaidica, M., Bentley, J. N., Patil, P. G., Mashour, G. A., & Chestek, C. A. (2016). Disruption of corticocortical information transfer during ketamine anesthesia in the primate brain. *NeuroImage, 134*, 459–465.

Silchenko, A. N., Adamchic, I., Pawelczyk, N., Hauptmann, C., Maarouf, M., Sturm, V., & Tass, P. A. (2010). Data-driven approach to the estimation of connectivity and time delays in the coupling of interacting neuronal subsystems. *Journal of Neuroscience Methods, 191*(1), 32–44.

Smith, V. A., Yu, J., Smulders, T. V., Hartemink, A. J., & Jarvis, E. D. (2006). Computational inference of neural information flow networks. *PloS Computational Biology, 2*(11), e161.

Therrien, C. W. (1992). *Discrete random signals and statistical signal processing*. Englewood Cliffs: Prentice Hall.

Vautard, R., Yiou, P., & Ghil, M. (1992). Singular-spectrum analysis: A toolkit for short, noisy chaotic signals. *Physica D: Nonlinear Phenomena, 58*(1), 95–126.

Venema, V., Ament, F., & Simmer, C. (2006). A stochastic iterative amplitude adjusted fourier transform algorithm with improved accuracy. *Nonlinear Processes in Geophysics, 13*(3), 321–328.

Vidal-Gadea, A. G., Jing, X., Simpson, D., Dewhirst, O. P., Kondoh, Y., Allen, R., & Newland, P. L. (2010). Coding characteristics of spiking local interneurons during imposed limb movements in the locust. *Journal of Neurophysiology, 103*(2), 603–615.

Vitanza, A., Patané, L., & Arena, P. (2015). Spiking neural controllers in multi-agent competitive systems for adaptive targeted motor learning. *Journal of the Franklin Institute, 352*(8), 3122–3143.

Watson, A. H., & Burrows, M. (1987). Immunocytochemical and pharmacological evidence for GABAergic spiking local interneurons in the locust. *Journal of Neuroscience, 7*(6), 1741–1751.

Wibral, M., Pampu, N., Priesemann, V., Siebenhühner, F., Seiwert, H., Lindner, M., & Vicente, R. (2013). Measuring information-transfer delays. *PloS One, 8*(2), e55809.

Wibral, M., Vicente, R., & Lindner, M. (2014). Transfer entropy in neuroscience. In *Directed Information Measures in Neuroscience* (pp. 3–36). Berlin Heidelberg: Springer.

Wilmer, A., de Lussanet, M., & Lappe, M. (2012). Time-delayed mutual information of the phase as a measure of functional connectivity. *PloS One, 7*(9), e44633.

Wollstadt, P., Martínez-Zarzuela, M., Vicente, R., Díaz-Pernas, F. J., & Wibral, M. (2014). Efficient transfer entropy analysis of non-stationary neural time series. *PloS One, 9*(7), e102833.

Yang, C., Jeannès, R. L. B., Faucon, G., & Shu, H. (2013). Detecting information flow direction in multivariate linear and nonlinear models. *Signal Processing, 93*(1), 304–312.